Probing two-dimensional Anderson localization without statistics

O. Leseur,[1] R. Pierrat,[1] J. J. Sáenz,[2,3] and R. Carminati[1,*]

[1]*ESPCI ParisTech, PSL Research University, CNRS, Institut Langevin, 1 rue Jussieu, F-75005, Paris, France*
[2]*Departmento de Física de la Materia Condensada, Instituto Nicolás Cabrera and Condensed Matter Physics Center (IFIMAC),*
Universidad Autónoma de Madrid, 28049 Madrid, Spain
[3]*Donostia International Physics Center (DIPC), Paseo Manuel Lardizabal 4, 20018 Donostia-San Sebastian, Spain*

We investigate the possibility of using the independence of the transmitted speckle pattern on the illumination condition as a signature of Anderson localization in a single configuration of a two-dimensional and open disordered medium. The analysis is based on exact numerical simulations of multiple light scattering. We introduce a similarity function that we propose as a reliable observable to probe Anderson localization without requiring any statistical averaging over an ensemble.

Initially proposed as an explanation for the metal-insulator transition in disordered solids [1], Anderson localization has become a concept at the center of wave physics, with impact far beyond solid-state physics [2,3]. Although the existence of localization in electronic transport has been clearly established [4], the search for convincing evidences of Anderson localization of other kinds of classical or quantum waves has remained an active area of research. The observation of localization has been reported in acoustics [5,6], for electromagnetic waves [7], matter waves [8], and in optics [9,10]. In optics, the observation of localization in three dimensions (3D) is still under debate due to the inherent presence of absorption [11], of nonlinearities [12], or the influence of polarization degrees of freedom [13].

Anderson localization cannot be described using classical transport theory, a wave theory being necessary to handle the interferences between multiply scattered amplitudes that induce localization. The scaling theory uses $\beta(g) = \partial \log g / \partial \log L$ as a central concept, with g the dimensionless conductance and L the size of the system [14]. It predicts different behaviors for different space dimensions [one-dimensional (1D) and two-dimensional (2D) systems are always localized while a phase transition is expected in 3D]. The so-called self-consistent theory provides a transport model for the averaged energy density, taking into account interferences between coherently multiply scattered waves [15]. Random matrix theory is another approach that in quasi-1D geometries (disordered waveguides) also predicts wave localization, based on computations of the statistical distribution of the transmission eigenvalues [16–19]. It is interesting to note that all quantities in these approaches are averaged over a set of realizations of a stochastic process that generates different configurations of the disorder medium (e.g., the spatial distribution of the potential or the position of the scattering centers). This is probably a consequence of the original observation of Anderson localization for electronic conduction, for which the only observable is the (self) averaged conductance. Since, at least for classical waves, it is possible to observe the wavefield in a given realization of the disordered

medium [20–22], one can question whether a signature of Anderson localization in a single realization of disorder can be found that does not require any statistical measurement. The purpose of this paper is to address this issue, based on simple theoretical arguments and exact numerical simulations of electromagnetic wave scattering in two dimensions.

In quasi-1D geometries (waveguides), it is known from random matrix theory that a discrete set of localized eigenmodes exists, that are all exponentially decaying in space [16–19]. In the localized regime (for a system with length L larger than the localization length ξ), only one eigenmode contributes to transmission, meaning that the transmitted speckle pattern reproduces the spatial dependence of this specific eigenmode. An important consequence is that the transmitted speckle pattern is independent on the illumination conditions. This feature of the localized regime in quasi-1D waveguide geometries has been observed in microwave experiments [23] and implications have been discussed in the context of wavefront shaping [24] or control of transmitted eigenchannels [25]. In this article we show that the independence of the transmitted speckle pattern on the illumination conditions in the localized regime holds for two-dimensional open systems, and we propose to use this property as a reliable signature of Anderson localization. The analysis is based on exact numerical simulations of multiple light scattering. First, we characterize the localized and the diffusive regimes by analyzing the spectrum of the transmitted intensity and of the local density of optical states (LDOS) inside the medium. Second, we introduce a similarity function that measures the invariance of the transmitted speckle pattern that we propose as an observable to probe Anderson localization in a single realization of a disordered medium.

The geometry of interest is depicted in Fig. 1. It consists of a finite size slab containing $N = 17\,500$ randomly distributed nonoverlapping scatterers, and illuminated by a Gaussian beam. The slab thickness is $L = 4.19 \times 10^{-5}$ m, and its transverse size is $D = 1.05 \times 10^{-4}$ m, which is chosen large compared to L. We consider TE-polarized waves with electric field parallel to the invariance axis of the 2D geometry, so that we can deal with a scalar field. The scatterers are described by their electric polarizability

$$\alpha(\omega) = -\frac{2\Gamma c^2}{\omega^2(\omega - \omega_0 + i\Gamma/2)}, \quad (1)$$
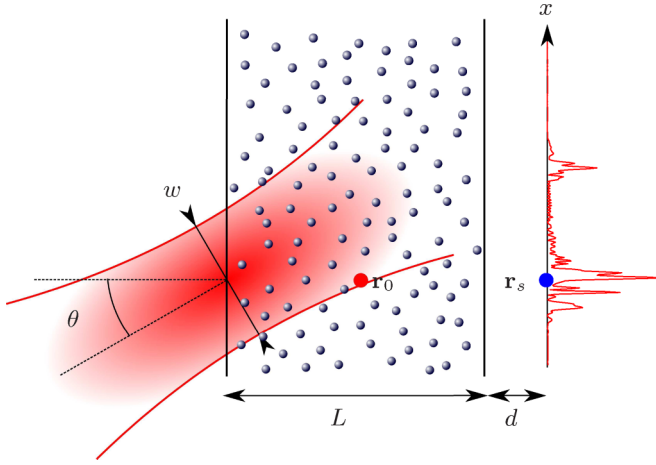
---

*remi.carminati@espci.fr

FIG. 1. (Color online) Sketch of the disordered medium. The incident Gaussian beam is focused on the input interface with an angle θ. $\mathbf{r}_0$ is a point inside the medium where the LDOS $\rho(\mathbf{r}_0,\omega)$ is computed. $\mathbf{r}_s$ is a point on the observation plane where the transmitted intensity $I(\mathbf{r}_s,\omega)$ is computed. The red solid line is an example of speckle pattern calculated in the observation plane.

where ω is the frequency and c is the speed of light in vacuum. This expression of the polarizability is consistent with the optical theorem (energy conservation) and is typical of a resonant scatterer with resonance frequency ω_0 and linewidth Γ. For the simulations we selected $\omega_0 = 3 \times 10^{15}$ s^{-1} and $\Gamma = 5 \times 10^{16}$ s^{-1}, so that the resonance has a low quality factor ensuring smooth variations of the scattering cross section over a large spectral width. The expression of the incident Gaussian beam reads

$$E_0(\mathbf{r},\omega) = \frac{E_0}{\sqrt{1+ia}} \exp\left[ik_0 r_\parallel - \frac{r_\perp^2}{w^2(1+ia)}\right], \quad (2)$$

with $a = 2r_\perp/(kw^2)$, $r_\parallel$ being the component of $\mathbf{r}$ along the direction of propagation and $r_\perp$ the transverse component of $\mathbf{r}$. The beam waist is $w = 2.1 \times 10^{-5}$ m, which is small compared to D, and the beam is focused at the center of the input interface. The direction of incidence is defined by the angle θ (see Fig. 1). In order to solve numerically the scattering problem, we use the coupled dipoles method [26]. The exciting field on scatterer number j is written as

$$E_j = E_0(\mathbf{r}_j,\omega) + \alpha(\omega)k_0^2 \sum_{\substack{k=1 \\ k \neq j}}^{N} G_0(\mathbf{r}_j - \mathbf{r}_k,\omega)E_k, \quad (3)$$

with $k_0 = \omega/c = 2\pi/\lambda$. The 2D scalar Green function G_0 connects a source dipole p at a position $\mathbf{r}'$ to the electric field $E(\mathbf{r})$ radiated at position $\mathbf{r}$ and is given by $G_0(\mathbf{r} - \mathbf{r}',\omega) = (i/4) H_0^{(1)}(k_0|\mathbf{r} - \mathbf{r}'|)$, where $H_0^{(1)}$ is the Hankel function of zero order and first kind. Equation (3) defines a set of N linear equations that are solved by a standard matrix inversion procedure. Once the exciting field is known on each scatterers, the field at any position $\mathbf{r}$ inside or outside the scattering

medium can be calculated using

$$E(\mathbf{r},\omega) = E_0(\mathbf{r},\omega) + \alpha(\omega)k_0^2 \sum_{k=1}^{N} G_0(\mathbf{r} - \mathbf{r}_k,\omega)E_k. \quad (4)$$

The first step consists of finding two frequency ranges corresponding to the diffusive and localized regimes, respectively, in a given realization of the disordered medium. The relevant parameters are the scattering mean free path ℓ, the optical thickness $b = L/\ell$, and the localization length ξ. For a 2D system, the localization length predicted from the self-consistent theory is $\xi = \ell \exp[\pi \, \mathrm{Re}(k_{\mathrm{eff}})\ell/2]$, where k_{eff} is the effective wave number of the medium [21,27]. For a rough estimate we can make the approximation $k_{\mathrm{eff}} \sim k_0 + i/(2\ell)$ and use the independent scattering mean free path $\ell = 1/(\rho\sigma)$, where $\sigma = k_0^3|\alpha(\omega)|^2/4$ is the scattering cross section. The two frequencies $\omega_c^l = 1.50 \times 10^{15}$ s^{-1} and $\omega_c^d = 2.70 \times 10^{15}$ s^{-1} can be used to define the center of two frequency intervals that correspond to the localized and the diffusive regimes, respectively. The corresponding wavelengths are $\lambda_c^l = 1.26 \times 10^{-6}$ m and $\lambda_c^d = 6.98 \times 10^{-7}$ m (all geometrical lengths such as system size L and D and incident beam waist w remain large compared to the wavelength). The mean free paths are $\ell(\omega_c^l) = 3.15 \times 10^{-7}$ m (giving a scattering strength $k_0\ell = 1.57$) and $\ell(\omega_c^d) = 5.66 \times 10^{-7}$ m (giving $k_0\ell = 5.10$). The optical thicknesses are $b(\omega_c^l) = 133$ and $b(\omega_c^d) = 74$, and the localization lengths are $\xi(\omega_c^l)/L \sim 0.09$ and $\xi(\omega_c^d)/L = 40$. This set of parameters shows that for both frequencies the system is in the multiple scattering regime, and that for the incident frequency ω_c^l it is expected to be localized, while for ω_c^d it is expected to be diffusive.

This prediction can be checked numerically. To do so we first compute the spectrum of the transmitted intensity $I(\mathbf{r}_s,\omega) = |E(\mathbf{r}_s,\omega)|^2$ at position $\mathbf{r}_s$ at a distance $d = 2\lambda_c$ from the output surface of the medium, as shown in Fig. 1, and for an illumination at normal incidence ($\theta = 0$). This specific distance has been chosen to ensure far-field detection (i.e., to avoid near-field effects). The intensity is calculated in different spectral ranges, corresponding to localization or diffusive transport, but in the same configuration of the disordered medium. The spectra $I(\mathbf{r}_s,\omega)$ are shown in Fig. 2 (blue solid line). In Fig. 2(a), corresponding to ω_c^l (localized regime), the spectrum exhibits strong fluctuations with many narrow peaks, each of them corresponding to one specific eigenfrequency. This is the expected behavior in the localized regime, where the mean spectral mode spacing $\Delta\omega$ is much larger than the mean mode linewidth $\delta\omega$, the dimensionless Thouless conductance being $g = \delta\omega/\Delta\omega \ll 1$. Conversely, in Fig. 2(b) corresponding to ω_c^d (diffusive regime), the spectrum is smooth, in agreement with the intuitive picture of a continuum of eigenmodes with $g = \delta\omega/\Delta\omega \gg 1$. To go further into the analysis, we have also computed the LDOS $\rho(\mathbf{r}_0,\omega)$ at a point $\mathbf{r}_0$ placed at the center of the medium. The LDOS is defined as

$$\rho(\mathbf{r}_0,\omega) = \frac{2\omega}{\pi c^2} \mathrm{Im}[G(\mathbf{r}_0,\mathbf{r}_0,\omega)], \quad (5)$$

where G is the Green function of the scattering medium. The Green function $G(\mathbf{r},\mathbf{r}_0,\omega)$ is deduced from a calculation of the electric field $E(\mathbf{r},\omega)$ based on Eq. (4), using a point dipole
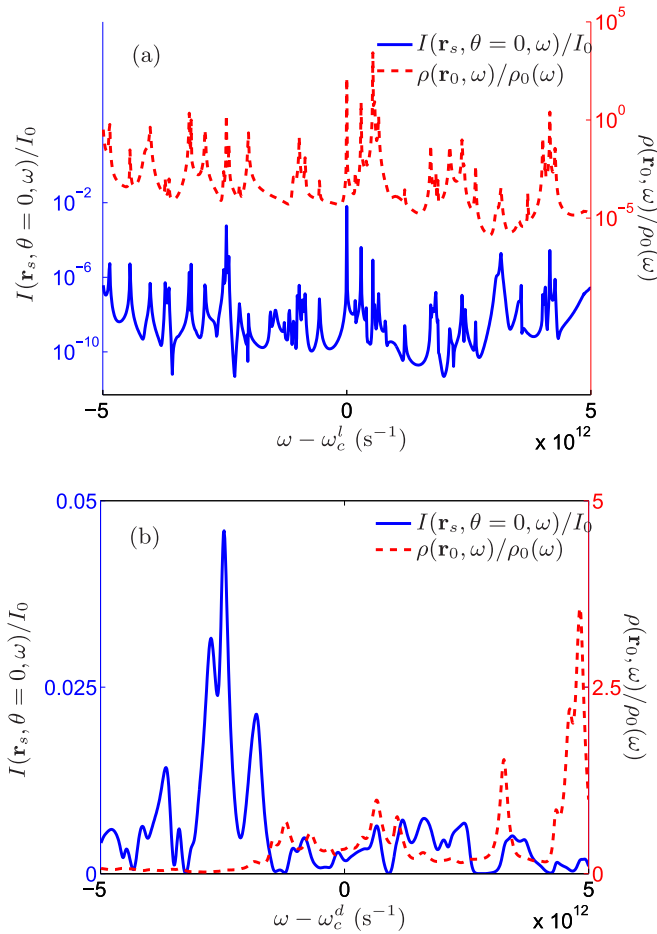
FIG. 2. (Color online) Normalized transmitted intensity spectrum $I(\mathbf{r}_s,\omega)/I_0$ for $\theta = 0$ (solid blue line) and normalized LDOS spectrum $\rho(\mathbf{r}_0,\omega)/\rho_0(\omega)$ (dashed red line) at a point placed at the center of the disordered region. (a) Localized regime. The spectrum is centered at frequency ω_c^l for which $\xi/L \sim 0.09$. (b) Diffusive regime. The spectrum is centered at frequency ω_c^d for which $\xi/L = 40$.

source dipole p placed at $\mathbf{r}_0$. The LDOS spectrum is also presented in Fig. 2 (red dashed line). In the localized regime [Fig. 2(a)], the LDOS spectrum is very similar to the intensity spectrum. Indeed, the one-to-one correspondence between spectral peaks confirms that they allow us to identify individual eigenmodes [28–30]. In the diffusive regime [Fig. 2(b)] the spectra of the LDOS and of the transmitted intensity are very different, due to the overlapping of several modes that contribute to transmission with different weights.

Since the localized and diffusive regimes have been characterized in the single configuration of the disordered medium, we can now proceed to the analysis of the speckle pattern produced in transmission in a plane at a distance d from the output surface. We show in Fig. 3 the spatial distribution of the intensity $I(x,\theta,\omega)$ for two values of the incidence angle θ. In the localized regime [Fig. 3(a)] we display the intensity profiles for $\theta = 0°$ and $\theta = 30°$ at frequency ω_c^l that has been chosen to coincide with a well pronounced peak in the transmission spectrum in Fig. 2(a). The intensity profiles are similar in shape (although they have a different amplitude before normalization). This result shows that, as in the quasi-
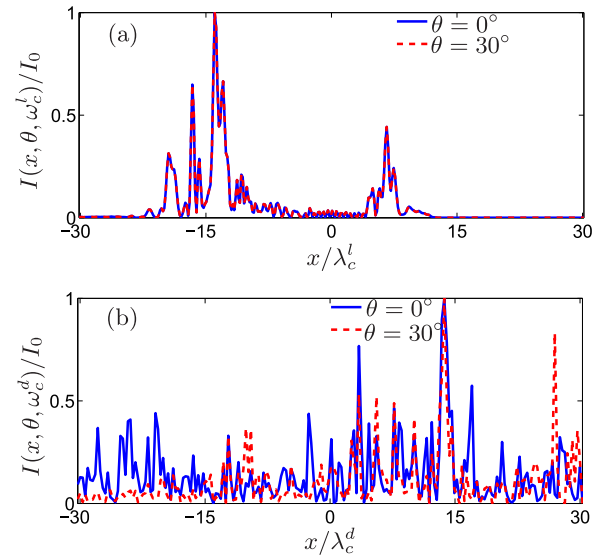

FIG. 3. (Color online) Normalized transmitted intensity $I(x,\theta,\omega)/I_0$ versus the normalized transverse direction x/λ in the localized regime [$\omega = \omega_c^l$, (a)] and in the diffusive regime [$\omega = \omega_c^d$, (b)] at normal incidence (solid blue line) and for an incidence angle $\theta = 30°$ (dashed red line).

1D geometry [18], one localized eigenmode dominates in transmission and imposes the spatial shape of the transmitted speckle. Therefore, this shape is independent on the incidence angle that only influences the coupling efficiency to the dominating eigenmode, changing only a constant prefactor in the speckle intensity. In the diffusive regime [Fig. 3(b)], the spatial intensity profiles are very different, with several nonoverlapping peaks. The transmitted speckle results from a weighted summation over many modes that becomes strongly dependent on the incidence angle (and more generally on the illumination conditions).

As a measure of the similarity between the speckle pattern obtained for an arbitrary incidence angle θ, and the reference speckle pattern obtained for $\theta = 0$, we define a similarity function $C(\theta,\omega)$ as follows:

$$C(\theta,\omega) = \frac{\int I(x,\theta=0,\omega)I(x,\theta,\omega)dx}{\sqrt{\int I(x,\theta=0,\omega)^2 dx \int I(x,\theta,\omega)^2 dx}} \qquad (6)$$

and we propose this quantity as a new and simple criterion to discriminate between the diffusive and the localized regimes in a single realization of a disordered medium. This definition is chosen so that $C(\theta,\omega) = 1$ if the normalized speckles are identical, and $C(\theta,\omega) < 1$ otherwise, as a consequence of the Cauchy-Schwarz inequality [31]. It is important to note that the definition of $C(\theta,\omega)$ does not involve any statistical averaging (it is not a correlation function as that usually defined to characterize the statistical properties of speckle patterns). Moreover, this spatial integration is not expected to replace a statistical average. In particular, there is no need for the integration range to cover a wide region that would be statistically representative. The integration is performed on a
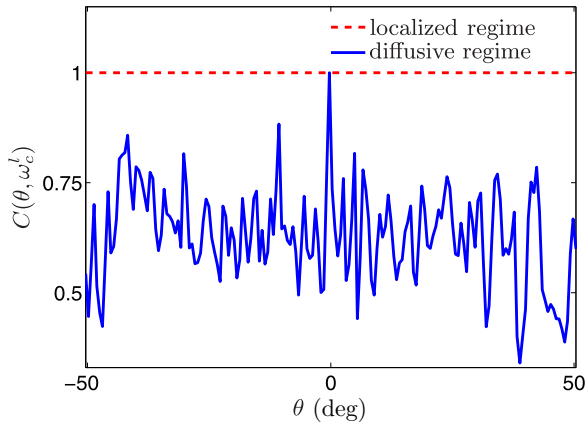
FIG. 4. (Color online) Similarity function $C(\theta,\omega)$ versus the incidence angle θ in the localized regime ($\omega = \omega_c^l$, dashed red line) and in the diffusive regime ($\omega = \omega_c^d$, solid blue line).

spatial range that is on the order of the transverse extent of the modes of the system.

In order to show that the similarity can be used to discriminate between the localized and the diffusive regime from the measurement of the transmitted speckle pattern in a single configuration of disorder, we plot in Fig. 4 the dependence of $C(\theta,\omega)$ on the incidence angle θ in the localized regime ($\omega = \omega_c^l$, dashed red line) and in the diffusive regime ($\omega = \omega_c^d$, solid blue line). In the localized regime the similarity function remains constant to a value close to unity, while it decreases very fast to stabilize around 0.6 is the diffusive regime. Although not shown, we have observed this behavior numerically in many different realizations of the disordered medium. The similarity function $C(\theta,\omega)$ thus appears as a reliable observable to discriminate between transport regimes in a single configuration of the disorder, without requiring any statistical analysis.

The relevance of a criterion based on a single realization of the disordered medium might be questioned, since in the usual statistical approach an underlying random process is assumed to create samples that belong either to the class of diffusive samples or to the class of localized samples, the distinction between both classes being made from the computation of averaged quantities (such as the Thouless conductance or the localization length). When considering a single configuration, one could think of it as an element belonging to both the ensemble created by a random process of the localized class, and the ensemble created by a random process of the diffusive class. Therefore, it seems paradoxical that the similarity function be able to discriminate between a localized or a diffusive sample without requiring any statistical averaging over an ensemble. The paradox is solved by realizing that a sample that would be at the intersection of the classes of localized and diffusive samples is very unlikely, and would not be found in practice.

In conclusion, we have investigated the Anderson localization regime in two dimensions in a single configuration of an open disordered medium. First, we have characterized the transport regime by computing and comparing the transmitted intensity and the LDOS spectra. We have observed a strong connection between both spectra in the localized regime reflecting the underlying spectral mode structure. Second, we have shown that a similarity function can be introduced that measures the change of the transmitted speckle pattern when the direction of incidence of the illuminating beam is changed. In the localization regime the similarity function remains close to one, while it decreases very fast with the incidence angle in the diffusive regime. This works opens new possibilities to probe two-dimensional Anderson localization without requiring any statistical averaging over an ensemble. An analysis of these results in terms of quasieigenmode expansions valid in open systems is beyond the scope of this study and left for future work.

[1] P. Anderson, Phys. Rev. **109**, 1492 (1958).

[2] P. Sheng, *Introduction to Wave Scattering, Localization and Mesoscopic Phenomena* (Academic, New York, 1995).

[3] A. Lagendijk, B. van Tiggelen, and D. S. Wiersma, Phys. Today **62**, 24 (2009).

[4] P. A. Lee and T. V. Ramakrishnan, Rev. Mod. Phys. **57**, 287 (1985).

[5] R. L. Weaver, Wave Motion **12**, 129 (1990).

[6] H. Hu, A. Strybulevych, J. H. Page, S. E. Skipetrov, and B. A. van Tiggelen, Nat. Phys. **4**, 945 (2008).

[7] A. A. Chabanov, M. Stoytchev, and A. Z. Genack, Nature (London) **404**, 850 (2000).

[8] J. Billy, V. Josse, Z. Zuo, A. Bernard, B. Hambrecht, P. Lugan, D. Clément, L. Sanchez-Palencia, P. Bouyer, and A. Aspect, Nature (London) **453**, 891 (2008).

[9] D. S. Wiersma, P. Bartolini, A. Lagendijk, and R. Righini, Nature (London) **390**, 671 (1997).

[10] G. Maret, T. Sperling, W. Bührer, A. Lubatsch, R. Frank, and C. M. Aegerter, Nat. Photon. **7**, 934 (2013).

[11] F. Scheffold, R. Lenke, R. Tweer, and G. Maret, Nature (London) **398**, 206 (1999).

[12] F. Scheffold and D. S. Wiersma, Nat. Photon. **7**, 934 (2013).

[13] S. E. Skipetrov and I. M. Sokolov, Phys. Rev. Lett. **112**, 023905 (2014).

[14] E. Abrahams, P. W. Anderson, D. C. Licciardello, and T. V. Ramakrishnan, Phys. Rev. Lett. **42**, 673 (1979).

[15] D. Vollhardt and P. Wölfle, Phys. Rev. B **22**, 4666 (1980).

[16] O. N. Dorokhov, Pis'ma Zh. Eksp. Teor. Fiz. **36**, 259 (1982) [JETP Lett. **36**, 318 (1982)].

[17] P. Mello, P. Pereyra, and N. Kumar, Ann. Phys. **181**, 290 (1988).

[18] C. W. J. Beenakker, Rev. Mod. Phys. **69**, 731 (1997).

[19] L. S. Froufe-Pérez, P. García-Mochales, P. A. Serena, P. A. Mello, and J. J. Sáenz, Phys. Rev. Lett. **89**, 246403 (2002).

[20] P. Sebbah, B. Hu, J. M. Klosner, and A. Z. Genack, Phys. Rev. Lett. **96**, 183902 (2006).

[21] D. Laurent, O. Legrand, P. Sebbah, C. Vanneste, and F. Mortessagne, Phys. Rev. Lett. **99**, 253902 (2007).

[22] F. Riboli, P. Barthelemy, S. Vignolini, F. Intonti, A. D. Rossi, S. Combrie, and D. S. Wiersma, Opt. Lett. **36**, 127 (2011).

[23] Z. Shi and A. Z. Genack, Phys. Rev. Lett. **108**, 043901 (2012).

[24] M. Davy, Z. Shi, J. Wang, and A. Z. Genack, Opt. Express **21**, 10367 (2013).

[25] A. Peña, A. Girschik, F. Libisch, S. Rotter, and A. A. Chabanov, Nat. Commun. **5**, 3488 (2014).

[26] M. Lax, Phys. Rev. **85**, 621 (1952).

[27] B. C. Gupta and Z. Ye, Phys. Rev. E **67**, 036606 (2003).

[28] L. Sapienza, H. Thyrrestrup, S. Stobbe, P. D. Garcia, S. Smolka, and P. Lodahl, Science **327**, 1352 (2010).

[29] J. Wang and A. Z. Genack, Nature (London) **471**, 345 (2011).

[30] A. Cazé, R. Pierrat, and R. Carminati, Phys. Rev. Lett. **111**, 053901 (2013).

[31] Other similarity functions can be defined, with vanishing value for two similar patterns. See http://www.scholarpedia. org/article/Similarity_measures